

Optimal selection of representative colors for spectral reflectance reconstruction in a multispectral imaging system

Hui-Liang Shen,^{1,*} Hong-Gang Zhang,¹ John H. Xin,^{2,3} and Si-Jie Shao²

¹Department of Information and Electronic Engineering, Zhejiang University, Hangzhou 310027, China

²Institute of Textiles and Clothing, Hong Kong Polytechnic University, Hong Kong, China

³E-mail: tcxinjh@inet.polyu.edu.hk

*Corresponding author: shenhl@zju.edu.cn

Received 28 January 2008; revised 6 March 2008; accepted 31 March 2008;
posted 3 April 2008 (Doc. ID 92181); published 29 April 2008

In a multispectral color imaging system, the spectral reflectance of the object being imaged always needs to be accurately reconstructed by employing the training samples on specific color charts. Considering that the workload is heavy when all those color samples are used in practical applications, it is important to select only a limited number of the most representative samples. This is possible as the color charts are usually designed to cover the range of commonly imaged colors, and the color samples are redundant for spectral image reconstruction. We propose an eigenvector-based method and a virtual-imaging-based method for representative color selection by minimizing the total reflectance root-mean-squares errors. The effectiveness of the proposed methods is confirmed by experimental results when compared with existing techniques. © 2008 Optical Society of America

OCIS codes: 110.4234, 330.1730, 330.1710.

1. Introduction

In the field of color imaging, multispectral imaging has been extensively studied in recent years. An important objective of a multispectral color imaging system is to transform the device-dependent camera response to the device-independent spectral reflectance, which is referred to as spectral characterization [1–6]. After spectral characterization, the reflectance of the object surface can be reliably reconstructed at a pixel scale spatial resolution. Several methods, such as Wiener estimation [1–3], pseudoinverse [4,5], and finite-dimensional modeling [4,6], have been studied for reflectance reconstruction. Among these methods, Wiener estimation is widely used as it can explicitly incorporate the correlation information of both spectral reflectance and imaging noise [1–3].

The mathematical transform for reflectance reconstruction is generally determined based on the imaging responses of all the color samples on standard and custom-made charts or even from Munsell chips [7]. The widely adopted color charts include the GretagMacbeth ColorChecker (MCC), the GretagMacbeth ColorChecker DC (CDC), and the American National Standards Institute (ANSI) IT8 charts. The MCC chart contains 24 colors, with 18 representing the colors of natural objects and six being grayscale ones. Both the CDC and IT8 charts include more than 200 colors. In spectral characterization it is possible that the accuracy of the mathematical transform determined by the 24 samples on the MCC chart is not optimal for other object colors. On the other hand, if all the colors on the CDC chart are employed, the workload becomes too heavy for practical applications. The solution to this problem is to select the most representative colors from the CDC chart or Munsell chips. Recently, Mohammadi *et al.* presented a color selection method by first grouping

0003-6935/08/132494-09\$15.00/0
© 2008 Optical Society of America

the similar samples into clusters and then choosing representative samples for the clusters based on vector angle analysis [8]. Cheung and Westland proposed four metric formulas to choose optimal colors for colorimetric characterization based on the criterion that the subsequent color to be selected into the representative color subset should be as different as possible from those already selected [9]. Hardeberg presented a method for significant color selection based on the criterion of minimum condition number (CN) to estimate the spectral sensitivity of an imaging system [4]. More specifically, he sought to minimize the ratio between the largest and smallest singular values of the selected reflectance subset. It is noted that the methods presented by Chueng and Westland [9] and Hardeberg [4] are both based on the similar assumption that the representative colors in the selected subset should be most distinct from each other.

In this study we propose two new color selection methods for spectral characterization under the criteria that the selected samples should produce minimum spectral root-mean-square (RMS) errors if they can optimally represent the whole color set. The first method, referred as the eigenvector-based (EV) one in this paper, tries to find the representative reflectance subset whose eigenvectors most accurately model the reflectances of the whole color set. The second method, referred as the virtual-imaging-based (VI) one, attempts to minimize the RMS errors between the actual reflectances and the estimated reflectances in a virtual multispectral imaging system. An experiment is conducted to evaluate the effectiveness of the proposed methods by using both synthetic data and real data.

The rest of this paper is organized as follows. Section 2 introduces the multispectral imaging process and the reflectance reconstruction based on Wiener estimation. Section 3 presents a color selection framework under which different methods can be unified. The proposed EV-based and VI-based color selection methods are described in Section 4. The experimental evaluation of the proposed and existing methods is presented in Section 5. Section 6 is the conclusion.

2. Reflectance Reconstruction by Using Wiener Estimation

A. Formulation of the Multispectral Imaging Process

A multispectral imaging system usually consists of a monochrome camera and a series of filters covering the visible spectrum from 400 to 700 nm. Without loss of generality, we suppose the camera response is proportional to the intensity of light entering the camera sensor and the visible spectrum is uniformly sampled into N samples. The multispectral imaging process can be represented using the matrix vector notation as follows:

$$\mathbf{v} = \mathbf{M}\mathbf{r} + \mathbf{b} + \mathbf{n}, \quad (1)$$

where \mathbf{v} is the $C \times 1$ vector of the camera responses, with C being the channel number; \mathbf{M} is the $C \times N$ matrix of spectral responsivity; \mathbf{r} is the $N \times 1$ vector of spectral reflectance; and \mathbf{b} and \mathbf{n} are the $C \times 1$ vectors of dark current response and imaging noise, respectively. It is noted that the spectral responsivity \mathbf{M} denotes the combined effect of the spectral power distribution of the imaging illuminant, the spectral transmittances of the filters, and the spectral sensitivity of the camera. By imaging a series of color patches with known reflectances, the terms \mathbf{M} and \mathbf{b} can be solved mathematically under the constraint of positive responsivity [10]. If we let $\mathbf{u} = \mathbf{v} - \mathbf{b}$, Eq. (1) becomes

$$\mathbf{u} = \mathbf{M}\mathbf{r} + \mathbf{n}. \quad (2)$$

B. Spectral Characterization by Wiener Estimation

The objective of spectral characterization of the multispectral imaging system is to convert the device-dependent camera response \mathbf{u} into the device-independent spectral reflectance \mathbf{r} . More precisely, we need to find an $N \times C$ matrix \mathbf{W} that transforms \mathbf{u} into the reconstructed reflectance $\hat{\mathbf{r}}$,

$$\hat{\mathbf{r}} = \mathbf{W}\mathbf{u}, \quad (3)$$

such that the spectral error between \mathbf{r} and $\hat{\mathbf{r}}$ is minimized. For Wiener estimation, the transform matrix \mathbf{W} is

$$\mathbf{W} = \mathbf{K}_r \mathbf{M}^T (\mathbf{M} \mathbf{K}_r \mathbf{M}^T + \mathbf{K}_n)^{-1}, \quad (4)$$

where the superscript T denotes matrix transpose and

$$\mathbf{K}_r = E\{\mathbf{r}\mathbf{r}^T\}, \quad (5)$$

$$\mathbf{K}_n = \text{diag}\{\sigma_1^2, \sigma_2^2, \dots, \sigma_C^2\}, \quad (6)$$

are the autocorrelation matrices of reflectance \mathbf{r} and noise \mathbf{n} , respectively. $E\{\cdot\}$ denotes the statistical expectation operator. We assume the noises of the channels are independent of each other and hence \mathbf{K}_n is a diagonal matrix. The noise variance of the c th ($1 \leq c \leq C$) channel can be computed as

$$\sigma_c^2 = E\{\|\mathbf{u}_c - \mathbf{m}_c \mathbf{r}\|^2\}, \quad (7)$$

where $\|\cdot\|$ denotes the Frobenius norm, \mathbf{u}_c represents the c th element of \mathbf{u} , and \mathbf{m}_c represents the c th row vector of \mathbf{M} .

3. Framework for Representative Color Selection

In this section we propose a framework for selecting the representative color subset Ω from the whole color set Θ for the purpose of reflectance reconstruction.

Under this framework the different color selection criteria can be unified by defining different object functions.

For clarity the reflectance in the subset Ω is denoted by \mathbf{s} and that in the set Θ is denoted by \mathbf{r} . We suppose L samples are ultimately selected from Θ as representatives, and use Ω_k ($1 \leq k \leq L$) to denote the subset containing k representative samples. First of all, we need to select the first color sample \mathbf{s}_1 of Ω_1 from the samples \mathbf{r}_j in Θ . Previous studies [4,9] showed that selecting the sample with maximum variance in spectral reflectance would be a good choice:

$$\Omega_1 = \{\mathbf{s}_1\}, \quad (8)$$

with

$$\mathbf{s}_1 = \arg \max_{\mathbf{r}_j \in \Theta} \|\mathbf{r}_j\|. \quad (9)$$

Suppose that after $k - 1$ times of selection, Ω_{k-1} contains $k - 1$ samples, i.e., $\mathbf{s}_1, \mathbf{s}_2, \dots$, and \mathbf{s}_{k-1} . Then the selection of the k th sample \mathbf{s}_k can be determined by minimizing an objective function J :

$$\mathbf{s}_k = \arg \min_{\mathbf{r}_j \in \Theta \cap \bar{\Omega}_{k-1}} J, \quad (10)$$

where $\bar{\Omega}_{k-1}$ is the complement of Ω_{k-1} . After the k th selection Ω is updated according to the following:

$$\Omega_k = \Omega_{k-1} \cup \{\mathbf{s}_k\}. \quad (11)$$

In this way, the color selection can be represented by the objective function J . For the CN-based method [4], J is defined as

$$J_{\text{CN}} = \frac{d_{\max}[\Omega_{k-1} \cup \{\mathbf{r}_j\}]}{d_{\min}[\Omega_{k-1} \cup \{\mathbf{r}_j\}]}, \quad \mathbf{r}_j \in \Theta \cap \bar{\Omega}_{k-1} \quad (12)$$

where matrix $[\Omega_{k-1} \cup \{\mathbf{r}_j\}] = [\mathbf{s}_1, \dots, \mathbf{s}_{k-1}, \mathbf{r}_j]$ and d_{\max} and d_{\min} are the maximum and minimum singular values of the matrix, respectively.

The object function J for the MAXSUMS metric proposed by Cheung and Westland [9] can be defined as

$$J_{\text{MAXSUMS}} = - \sum_{i=1}^{k-1} \|\mathbf{r}_j - \mathbf{s}_i\|^{1/2}, \quad (13)$$

$$\mathbf{s}_i \in \Omega_{k-1}, \mathbf{r}_j \in \Theta \cap \bar{\Omega}_{k-1}.$$

Note that the first minus notation “-” in Eq. (13) is used to convert the “maximum” operation to the “minimum” one. The objective functions of other three metrics (MAXMINS, MAXSUMC, and MAXMINC) [9] can be defined in similar ways. Our investigation indicates MAXSUMS is the best one among these four metrics in spectral characterization.

After all the needed L representative samples are selected, the transform matrix $\mathbf{W}_{s,L}$ of Wiener estimation using these representative training colors becomes

$$\mathbf{W}_{s,L} = \mathbf{K}_{s,L} \mathbf{M}^T (\mathbf{M} \mathbf{K}_{s,L} \mathbf{M}^T + \mathbf{K}_n)^{-1}, \quad (14)$$

where $\mathbf{K}_{s,L}$ is the autocorrelation matrix of the representative reflectances

$$\mathbf{K}_{s,L} = E\{\mathbf{s}\mathbf{s}^T\}, \quad \mathbf{s} \in \Omega_L. \quad (15)$$

4. Proposed Methods

It is worthwhile to mention that the objective functions in Eqs. (12) and (13) of the existing methods try to select the most distinct samples under their respective metrics. We argue that, as the selected representative samples are used for spectral characterization, they should be the most “representative” ones under the criteria of minimum spectral errors in reflectance reconstruction. Based on this consideration, we propose two new methods for representative color selection.

A. EV-Based Color Selection

In the EV-based method, the representative color is selected based on the criterion that the eigenvectors of the subset Ω_k should cover most of the reflectance characteristics of the whole set Θ . To compute the eigenvectors of $\Omega_{k-1} \cup \{\mathbf{r}_j\}$, we apply singular value decomposition (SVD) [11] as follows:

$$\mathbf{U} \mathbf{D} \mathbf{V}^T = [\Omega_{k-1} \cup \{\mathbf{r}_j\}], \quad \mathbf{r}_j \in \Theta \cap \bar{\Omega}_{k-1}, \quad (16)$$

where \mathbf{U} is an $N \times N$ column-orthogonal matrix, \mathbf{D} is a $N \times k$ matrix with nonzero singular values in its diagonal elements and zeros elsewhere, and \mathbf{V} is a $k \times k$ column-orthogonal matrix. The matrix \mathbf{U} is composed of N eigenvectors of the symmetric matrix $[\Omega_{k-1} \cup \{\mathbf{r}_j\}] [\Omega_{k-1} \cup \{\mathbf{r}_j\}]^T$. If the selected k samples are representative, the most important P eigenvectors associated with the P largest singular component values should be able to represent the reflectance $\mathbf{r} \in \Theta$ accurately [3,12,13]. Our investigation indicates that color accuracy of the EV-based method does not change significantly when the value of P varies from 10 to 20. In this regard, we use $P = 15$ in the experiment.

For a reflectance $\mathbf{r} \in \Theta$, it can be represented by the $p = \min(k, P)$ most important eigenvectors as

$$\mathbf{r} = \mathbf{U}_p \mathbf{a}, \quad (17)$$

where \mathbf{U}_p is the $N \times p$ matrix composed of the p eigenvectors and \mathbf{a} is the corresponding $p \times 1$ coefficient vector, which can be easily solved as

$$\mathbf{a} = \mathbf{U}_p^+ \mathbf{r}, \quad (18)$$

where the superscript $+$ denotes matrix pseudoinverse. By substituting Eq. (18) into Eq. (17), the

estimate of reflectance \mathbf{r} can be computed as

$$\hat{\mathbf{r}}_{\text{EV}} = \mathbf{U}_p \mathbf{a} = \mathbf{U}_p \mathbf{U}_p^+ \mathbf{r}. \quad (19)$$

If the eigenvector matrix \mathbf{U}_p represents the reflectance $\mathbf{r} \in \Theta$ accurately, $\hat{\mathbf{r}}_{\text{EV}}$ should be very close to \mathbf{r} . Based on this point, the objective function of the EV-based color selection is defined as

$$J_{\text{EV}} = E\{\|\hat{\mathbf{r}}_{\text{EV}} - \mathbf{r}\|\} = E\{\|(\mathbf{U}_p \mathbf{U}_p^+ - \mathbf{I})\mathbf{r}\|\}, \quad (20)$$

where \mathbf{I} is the $N \times N$ identity matrix. It is noted that the objective function in Eq. (20) does not depend upon the multispectral imaging system.

B. VI-Based Color Selection

If the corresponding camera response \mathbf{u} for each reflectance $\mathbf{r} \in \Theta$ is known, the spectral RMS error for the objective function can be computed between the actual reflectance and the reconstructed reflectance in Eq. (4). However, the camera responses of the reflectances $\mathbf{r} \in \Theta$ are unknown at the stage of color selection, and only the representative samples will be imaged for the subsequent spectral characterization. Our solution is to build a VI system with virtual spectral responsivity \mathbf{M}_{VI} so that the virtual response \mathbf{u}_{VI} for a reflectance $\mathbf{r} \in \Theta$ is computed as

$$\mathbf{u}_{\text{VI}} = \mathbf{M}_{\text{VI}} \mathbf{r}. \quad (21)$$

In this study we assume \mathbf{M}_{VI} is of narrowband, and the first and N th filters (corresponding to 400 and 700 nm wavelength, respectively) are included in all filter combinations. For a multispectral imaging system with C channels, the channel interval

$$Q = \frac{N-1}{C-1}, \quad (22)$$

and the filter index of the c th ($1 \leq c \leq C$) channel is

$$q(c) = 1 + Q(c-1). \quad (23)$$

Table 1 gives the corresponding values of the channel interval Q and the filter index $q(c)$ for different channel numbers C .

Although the spectral transmittances of actual narrowband filters are generally of approximate Gaussian shapes [14], we assume those of the virtual imaging system are of quite simple forms:

Table 1. Interval Value Q and Filter Index $q(c)$ for Different Channel Numbers C

Channel number C	Interval Q	Filter index $q(c)$
6	6	1,7,13,19,25,31
11	3	1,4,7,10,13,16,19,22,25,28,31
16	2	1,3,5,7,9,11,13,15,17,19,21,23,25,27,29,31

$$M_{\text{VI}}(c,j) = \begin{cases} 1 & j \in [\max(q(c)-1, 1), \min(q(c)+1, N)] \\ 0 & \text{otherwise} \end{cases}, \quad (24)$$

where $1 \leq c \leq C$ and $1 \leq j \leq N$. Equation (24) means that the spectral responsivities of the c th channel are 100% at the position $q(c)$ and its adjacent left and right sides and 0% elsewhere. For illustration Fig. 1 plots the shapes of \mathbf{M}_{VI} with six and 11 channels. As can be observed from Eq. (24) and Fig. 1, the bandwidths of the VI spectral responsivities of the first and C th channels are 20 nm and those of other channels are 30 nm.

For the spectral characterization of the VI system we compute the autocorrelation matrix of the selected representative reflectances in set $\Omega_{k-1} \cup \{\mathbf{r}_j\}$:

$$\mathbf{K}_{s,k} = E\{\mathbf{s}\mathbf{s}^T\}, \quad \mathbf{s} \in \Omega_{k-1} \cup \{\mathbf{r}_j\}, \quad (25)$$

where $\mathbf{r}_j \in \Theta \cap \bar{\Omega}_{k-1}$. The reflectance of the VI system

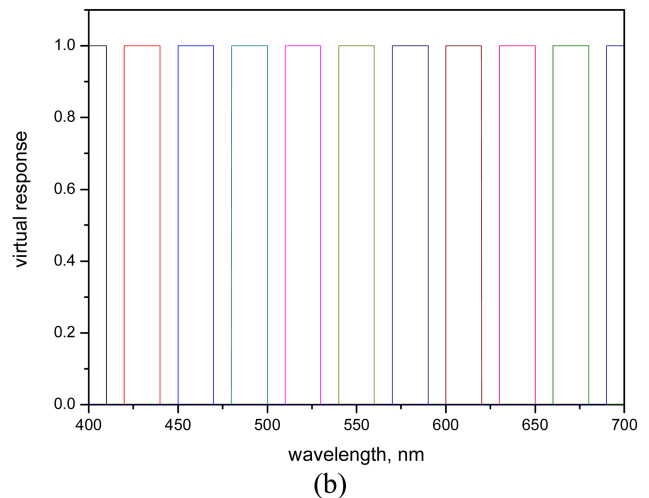
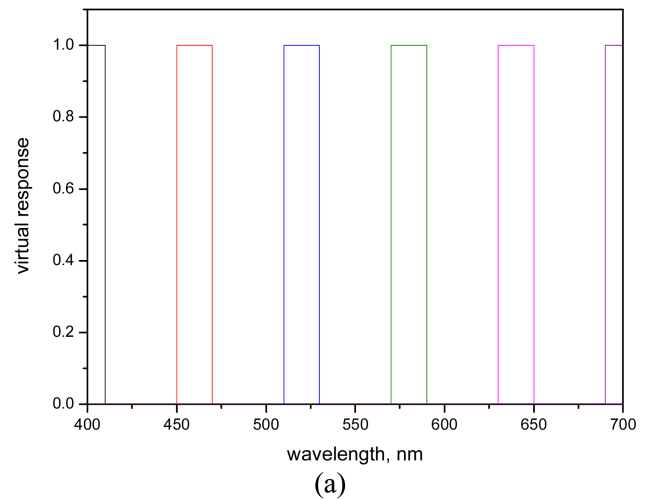


Fig. 1. (Color online) Virtual spectral responsivity of (a) six channels and (b) 11 channels.

can be estimated using Wiener estimation without the consideration of imaging noise:

$$\begin{aligned}\hat{\mathbf{r}}_{\text{VI}} &= \mathbf{K}_{s,k} \mathbf{M}_{\text{VI}}^T (\mathbf{M}_{\text{VI}} \mathbf{K}_{s,k} \mathbf{M}_{\text{VI}}^T)^{-1} \mathbf{u}_{\text{VI}} \\ &= \mathbf{K}_{s,k} \mathbf{M}_{\text{VI}}^T (\mathbf{M}_{\text{VI}} \mathbf{K}_{s,k} \mathbf{M}_{\text{VI}}^T)^{-1} \mathbf{M}_{\text{VI}} \mathbf{r}.\end{aligned}\quad (26)$$

Then the objective function of the VI-based color selection is

$$\begin{aligned}J_{\text{VI}} &= E\{\|\hat{\mathbf{r}}_{\text{VI}} - \mathbf{r}\|\} \\ &= E\{\|(\mathbf{K}_{s,k} \mathbf{M}_{\text{VI}}^T (\mathbf{M}_{\text{VI}} \mathbf{K}_{s,k} \mathbf{M}_{\text{VI}}^T)^{-1} \mathbf{M}_{\text{VI}} - \mathbf{I})\mathbf{r}\|\}.\end{aligned}\quad (27)$$

5. Experiment and Discussion

The multispectral color imaging system used in this study includes a monochrome digital camera manufactured by QImaging and a liquid-crystal tunable filter (LCTF) made by Cambridge Research and Instrument. The relative spectral transmittances of the 31 filters in the range of 400–700 nm are shown in Fig. 2. For the peak wavelengths less than 440 nm the filters contain much noise, which indicates that the filters are not ideal. The multispectral images of the CDC chart were acquired using the imaging system under an approximate D65 lighting condition. The spectral reflectances of the color patches on the MCC and CDC charts were measured using a GretagMacBeth spectrophotometer model 7000A. In total, 198 colors on the CDC chart were used in the experiment, excluding the glossy ones and the duplicated darkest ones. The reflectances of 1269

Munsell color chips were obtained from the website <http://spectral.joensuu.fi> and were resampled at a 10 nm interval. We did not acquire the multispectral images of the MCC charts and Munsell chips using the actual imaging system as these two targets were only used for computer simulation.

In the experiment different channel numbers, i.e., 6, 11, and 16, were used. Table 1 shows the channel intervals and filter indices of different channel numbers. The evaluations of color selection methods were conducted on two different datasets, i.e., the synthetic one and the real one. In the synthetic dataset part, we investigated the influence of different levels of imaging noise and different channel combinations as well. In the real dataset part, only the influence of different channel combinations was studied. The performances of the color selection methods were evaluated in terms of the color accuracy of the Wiener estimation-based spectral characterization. For a thorough comparison, we also conducted spectral characterization using the 198 CDC colors, the 1296 Munsell charts, and the 24 MCC colors in the experiment. Table 2 shows the color targets used in the experiment parts using synthetic and real datasets.

To evaluate the color accuracy of spectral characterization quantitatively the spectral RMS error between the actual and reconstructed reflectances is computed as

$$\text{RMS} = \|\hat{\mathbf{r}} - \mathbf{r}\|. \quad (28)$$

The colorimetric error ΔE_{00} is computed according to the CIEDE2000 color difference formula [15] for the

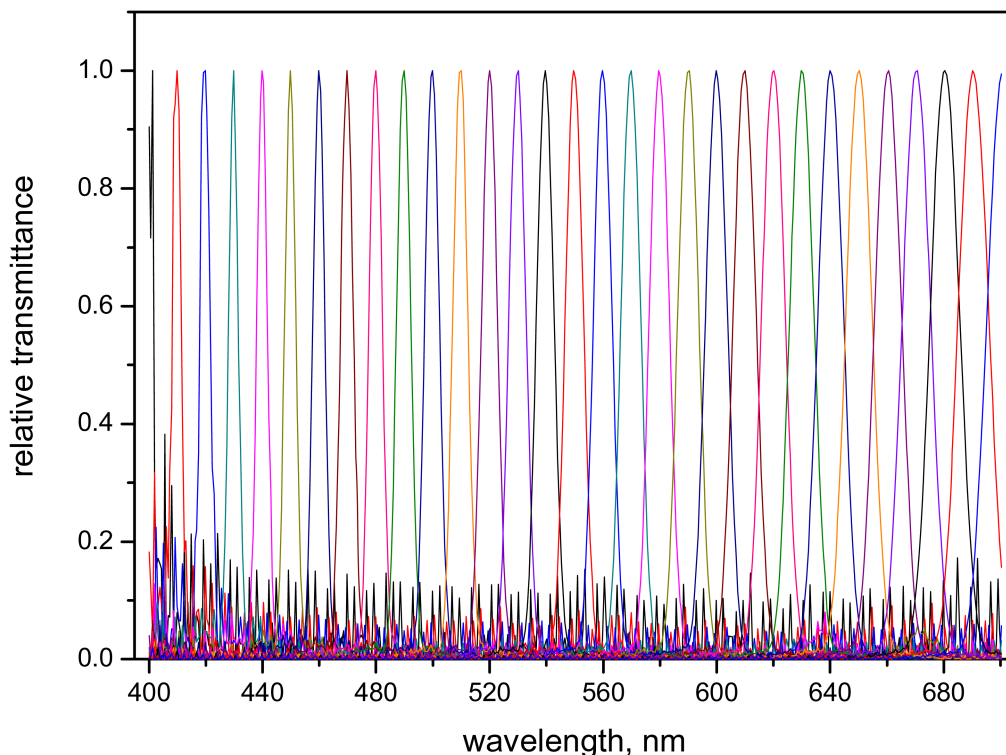


Fig. 2. (Color online) Relative spectral transmittance of the liquid-crystal tunable filter.

Table 2. Training and Testing Color Targets in the Synthetic and Real Datasets

	Training color target	Test color target
Synthetic dataset part	Munsell	Munsell, MCC
Real dataset part	CDC	CDC

1964 CIE 10° standard observer under the standard illuminants D65 and F2.

A. Synthetic Dataset Part

In the synthetic dataset part the color selection methods are evaluated on the Munsell chips. The spectral responsivity \mathbf{M} of the imaging system is assumed to be known *a priori* and the synthetic response \mathbf{u}_{syn} of the Munsell chips is simulated as

$$\mathbf{u}_{\text{syn}} = \mathbf{M}\mathbf{r} + \mathbf{n}_\sigma, \quad (29)$$

where \mathbf{n}_σ denotes Gaussian noise with zero mean and variance σ^2 . Note that the spectral responsivity \mathbf{M} in Eq. (29) is the one presolved from the real multispectral system. The corresponding signal-to-noise ratio (SNR) is

$$\text{SNR} = 10 \log \left(\frac{\text{Tr}(\mathbf{M}\mathbf{K}_r\mathbf{M}^T)}{\sigma^2} \right), \quad (30)$$

where the term $\text{Tr}(\mathbf{M}\mathbf{K}_r\mathbf{M}^T)$ is the average signal power captured by the simulated multispectral imaging system. In this study the synthetic responses are simulated under the noise level $\text{SNR} = \infty$ and 50, respectively.

Figure 3 illustrates the relationship between spectral RMS error of reflectance reconstruction and the number of representative colors L . It is found that the spectral error is relatively stable when L varies from 25 to 80. This trend is similar to the findings of Mohammadi *et al.* [8]. As the MCC chart contains 24

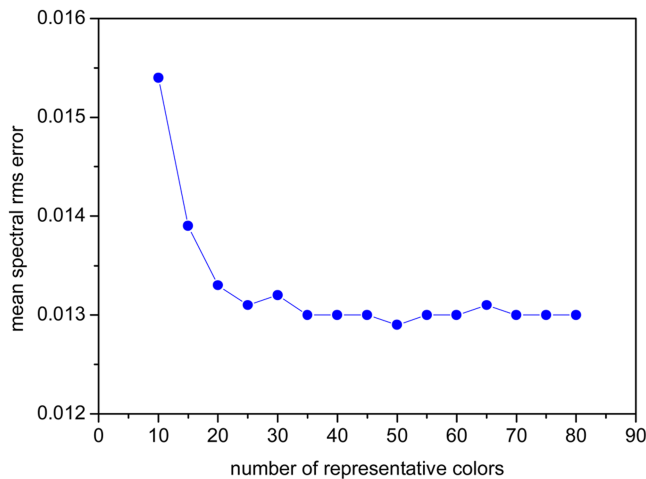


Fig. 3. (Color online) Distribution of mean spectral RMS error with respect to the number of representative colors in the combination of $C = 6$ and $\text{SNR} = 50$.

samples we let $L = 24$ in the experiment for convenience of comparison. Figure 4 shows the average spectral RMS errors and ΔE_{00} errors (under D65) for all of the methods mentioned under different combinations of channel number C and SNR value. It is clear that when C is fixed, the multispectral imaging system with a higher SNR will produce a more accurate reflectance reconstruction for each method. As expected, the spectral and colorimetric errors decrease with respect to the increasing of C value. It is interesting to observe that the color errors fall rapidly when C changes from 6 to 11. However, this effect is not so obvious between the channel numbers 11 and 16. Take the EV-based method under the condition of $\text{SNR} = \infty$ for an example. The improved spectral accuracy is 0.008 (=0.0125–0.0045) when C changes from 6 to 11, but it is only 0.0015 (= 0.0045–0.0030) when C varies from 11 to 16. In this regard, we consider that the multispectral imaging system with 11 narrowband filters can produce acceptable reflectance reconstruction.

It is also clear that under each combination of C and SNR the proposed EV-based and VI-based methods are more efficient than the MCC and MAX-SUMS methods. This indicates that the selected 24 representative colors according to the proposed methods outperform the usually adopted MCC target. In most cases the mean spectral and colorimetric errors of the two proposed methods are lower than the CN-based method. The only exception is the combination of $C = 16$ and $\text{SNR} = 50$.

B. Real Dataset Part

In the real dataset part of the experiment the color selection methods are evaluated on the actual imaging responses of the 198 colors on the CDC chart. The spectral responsivity of the imaging system was also mathematically recovered from the selected representative samples. The spectral RMS errors and color difference errors of the reflectance reconstruction are listed in Table 3. It is found that for all of the different channel combinations the mean spectral errors of the two proposed methods are the lowest among all methods (except the one using all samples). The proposed methods also outperform the CN-based method in the cases of $C = 6$ and 11 in terms of mean colorimetric errors. In the case of 16 channels, however, the mean colorimetric errors of the proposed methods are higher than those of the CN-based method. This is unsurprising as the improvement of the VI-based method over the CN method is only 0.0008 in terms of spectral RMS error. Because of the nonlinear transform between reflectance and CIELAB color space and the complicated calculation in the CIEDE2000 formula, this increased magnitude of spectral accuracy cannot ensure the improvement of colorimetric accuracy. Figure 5 shows the reconstructed reflectances using the different color selection methods when $C = 11$. It is observed that although the reconstructed reflectances of the proposed two methods do not match the actual ones

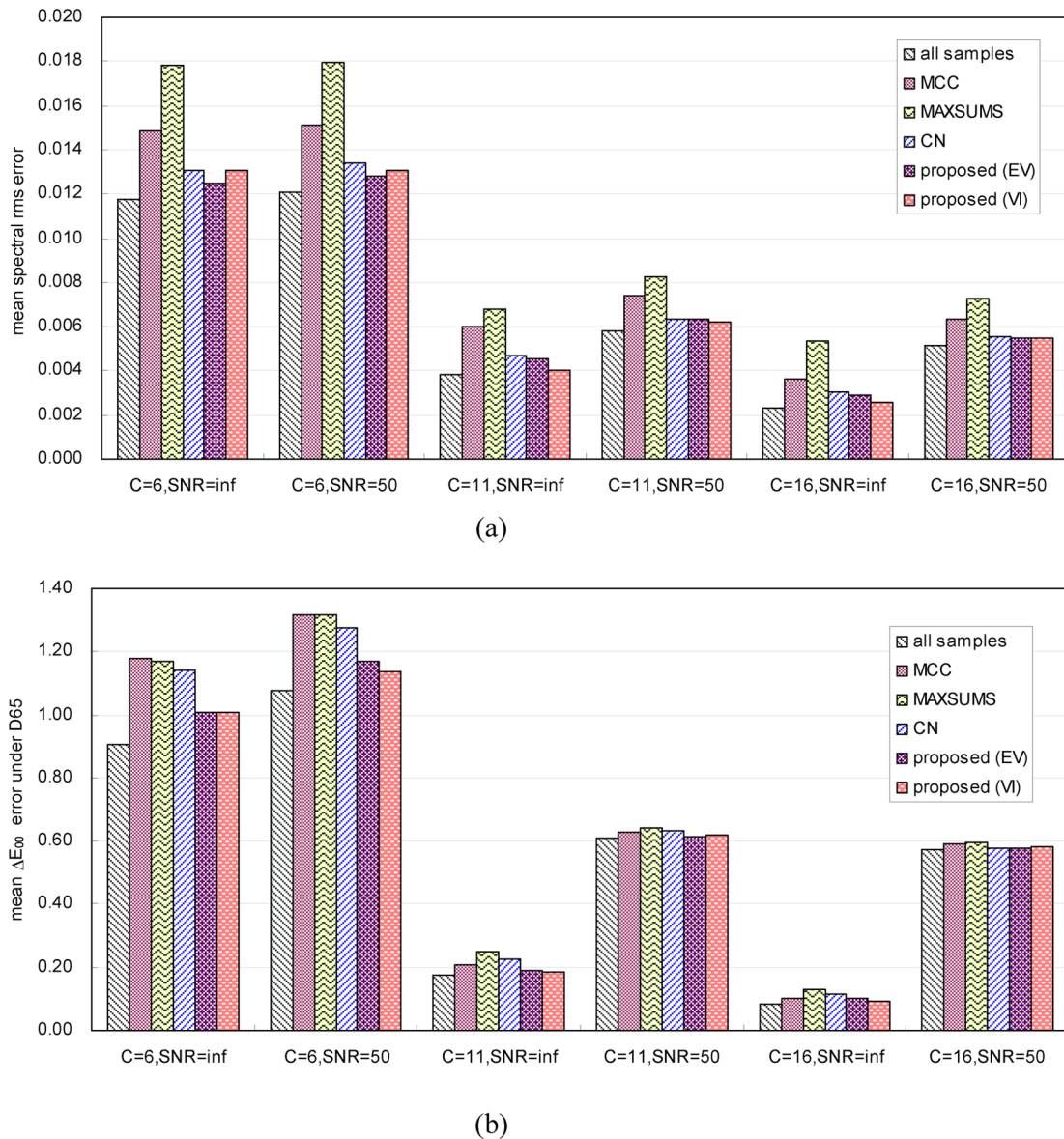


Fig. 4. (Color online) (a) Mean spectral RMS errors and (b) mean ΔE_{00} errors under D65 of different methods when applied on the synthetic dataset.

perfectly they are the best ones when compared with other methods. These findings are consistent with those obtained from the experiment using the synthetic dataset.

6. Conclusion

The accurate construction of spectral reflectance is an important objective for a multispectral color imaging system. We proposed two methods for the selection of representative color samples for spectral characterization by minimizing the spectral RMS errors of the whole color set. The first method selects the representative samples whose eigenvectors can accurately model the reflectance set, while the second method attempts to find the representative

samples that minimize the actual and estimated reflectances of a virtual-imaging system. Experiments were conducted to evaluate the different color selection methods in the cases of different channel combinations, using both a synthetic dataset and a real dataset. It was shown that the two proposed methods are effective when compared with other existing methods in terms of both spectral and colorimetric errors.

It is noted that the performance of the proposed color selection methods are evaluated by only three color sets in this study. However, due to different materials and pigment composition, the reflectance characteristics of other objects may be different from those in this study. In future work we will investigate

Table 3. Spectral RMS Errors and Colorimetric Errors of Different Color Selection Methods when Using Real Data of 198 Colors on the CDC Chart

C	Method	Spectral RMS			ΔE_{00} under D65			ΔE_{00} under F2		
		Mean	Std.	Max.	Mean	Std.	Max	Mean	Std.	Max
6	All samples	0.0170	0.0095	0.0567	1.54	1.07	6.23	1.81	1.21	7.02
	MAXSUMS	0.0278	0.0347	0.3149	3.67	6.11	57.74	4.31	6.55	52.84
	CN	0.0195	0.0117	0.0726	1.84	1.17	6.91	2.14	1.26	6.77
	Proposed (EV)	0.0184	0.0105	0.0658	1.59	1.13	7.07	1.98	1.35	7.16
	Proposed (VI)	0.0181	0.0116	0.0712	1.81	1.49	8.76	2.02	1.66	9.57
11	All samples	0.0079	0.0043	0.0278	0.79	0.52	3.30	0.81	0.51	2.78
	MAXSUMS	0.0121	0.0068	0.0406	1.33	0.92	6.50	1.44	1.00	7.28
	CN	0.0107	0.0062	0.0322	1.22	0.78	4.74	1.28	0.78	3.80
	Proposed (EV)	0.0090	0.0066	0.0388	0.98	0.69	4.44	0.98	0.68	4.20
	Proposed (VI)	0.0089	0.0055	0.0319	0.88	0.62	3.75	0.89	0.67	5.19
16	All samples	0.0065	0.0040	0.0276	0.71	0.47	3.02	0.71	0.45	2.61
	MAXSUMS	0.0147	0.0131	0.1082	2.00	2.78	34.62	2.20	3.09	39.29
	CN	0.0090	0.0070	0.0329	0.96	0.66	4.21	0.98	0.63	3.59
	Proposed (EV)	0.0094	0.0083	0.0430	1.12	1.12	8.91	1.12	1.19	9.55
	Proposed (VI)	0.0082	0.0057	0.0349	1.03	1.00	8.60	1.03	0.96	8.24

^aThe minima of the average color errors of the four methods (MAXSUMS, CN, EV, and VI) are in bold type.

the representative color selection and spectral characterization using other typical materials, such as plastics and textiles.

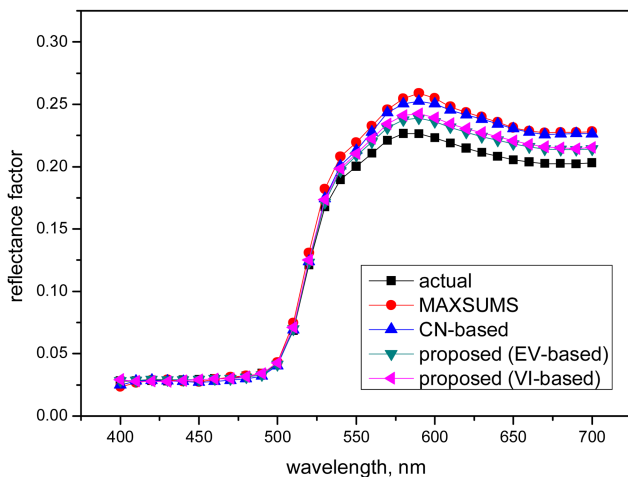
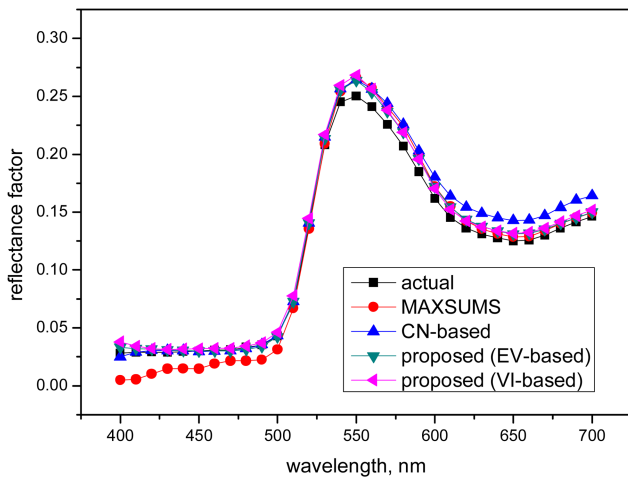


Fig. 5. (Color online) Reflectance reconstruction of different color selection methods.

We thank the anonymous reviewers for their constructive comments that have helped to improve the presentation of this paper. This work has been supported by the National Natural Science Foundation of China under grant 60 602 027 and the Hong Kong Research Institute of Textiles and Apparel (HKRITA) under grant ITP/009/07TP.

References

1. Y. Murakami, T. Obi, M. Yamaguchi, N. Ohyama, and Y. Komiya, "Spectral reflectance estimation from multi-band image using color chart," *Opt. Commun.* **188**, 47–54 (2001).
2. N. Shimano, "Recovery of spectral reflectance of objects being imaged without prior knowledge," *IEEE Trans. Image Process.* **15**, 1848–1856 (2006).
3. H. L. Shen, P. Q. Cai, S. J. Shao, and J. H. Xin, "Reflectance reconstruction for multispectral imaging by adaptive Wiener estimation," *Opt. Express* **15**, 15545–15554 (2007).
4. J. Y. Hardeberg, "Acquisition and reproduction of color images: colorimetric and multispectral approaches" (Universal Publishers, 2001), dissertation.com.
5. J. Y. Hardeberg, F. Schmitt, and H. Brettel, "Multispectral color image capture using liquid crystal tunable filter," *Opt. Eng.* **41**, 2532–2548 (2002).
6. V. Cheung, S. Westland, C. Li, J. Hardeberg, and D. Connah, "Characterization of trichromatic color cameras by using a new multispectral imaging technique," *J. Opt. Soc. Am. A* **22**, 1231–1240 (2005).
7. J. P. S. Parkkinen, J. Hallikainen, and T. Jaaskelainen, "Characteristic spectra of Munsell colors," *J. Opt. Soc. Am. A* **6**, 318–322 (1989).
8. M. Mohammadi, M. Nezamabadi, R. S. Berns, and L. A. Taplin, "Spectral imaging target development based on hierarchical cluster analysis," in *Proceedings of Twelfth Color Imaging Conference: Color Science and Engineering, Systems, Technologies and Applications*, (IS&T, 2004), pp. 59–64.
9. V. Cheung and S. Westland, "Methods for optimal color selection," *J. Imaging Sci. Technol.* **50**, 481–488 (2006).
10. K. Barnard and B. Funt, "Camera characterization for color research," *Color Res. Appl.* **27**, 152–163 (2002).
11. W. H. Press, S. A. Teukolsky, W. T. Vetterling, and B. P. Flannery, *Numerical Recipes in C: The Art of Scientific Computing*, 2nd Ed. (Cambridge University Press, 1992).

12. L. Maloney, "Evaluation of linear models of surface spectral reflectance with small number of parameters," *J. Opt. Soc. Am. A* **3**, 1673–1683 (1986).
13. M. J. Vrhel, R. Gershon, and L. S. Iwan, "Measurement and analysis of object reflectance spectra," *Color Res. Appl.* **19**, 4–9 (1994).
14. M. G. A. Thomson and S. Westland, "Colour-imager calibration by parametric fitting of sensor responses," *Color Res. Appl.* **26**, 442–449 (2001).
15. M. L. Luo, G. Cui, and B. Rigg, "The development of the CIE 2000 colour-difference formula: CIEDE2000," *Color Res. Appl.* **26**, 340–350 (2001).